Research Article Vol. 4, No. 5 / 15 May 2021 / OSA Continuum 1545

Resonance-affected high-order harmonic emission from atomic and molecular chromium laser-induced plasmas

RASHID A. GANEEV[1,2,3,4,*] AND HIROTO KURODA[1,5,6]

[1]Saitama Medical University, Saitama 350-0495, Japan
[2]Institute of Astronomy, University of Latvia, Riga, LV – 1586, Latvia
[3]Department of Physics, Voronezh State University, Voronezh 394006, Russia
[4]Moscow Institute of Physics and Technology, Dolgoprudny 141701, Russia
[5]Advanced Laser Technology Inc., Tama-city, Tokyo 206-0014, Japan
[6]Aichi Medical University, Nagakute-city 480-1195, Japan
[*]rashid_ganeev@mail.ru

Abstract: The resonance enhancement of single-harmonic emission during the propagation of ultrafast pulses through chromium-contained plasmas is reexamined. We compare atomic (Cr) and molecular (Cr_2O_3, Cr_3C_2) plasmas to demonstrate a distinction in the enhancement factor of the single harmonic. We show how, in the case of 806 nm pump, the enhancement of the 29^{th} harmonic (λ=27.8 nm) in Cr-contained plasma depends on the constituency of the plasma components at different conditions of target ablation. The application of tunable (1280–1440 nm) radiation allows the demonstration of notable variations of single harmonic (46 to 49 orders) enhancement using a two-color pump of Cr-contained plasma.

1. Introduction

The resonance-induced enhancement of harmonics during propagation of ultrafast pulses through the laser-induced plasma (LIP) allows improving the high-order harmonic generation (HHG) efficiency and increasing the yield of coherent emission in the extreme ultraviolet (XUV) range. The demonstration of resonance enhancement of harmonics, quasi-phase matching of different groups of harmonics, nanoparticle-induced growth of harmonic yield, etc. has revealed the attractive features of LIP as the efficient medium for generation of high-order harmonics [1–5]. Particularly, the resonance processes were systematically analyzed using In, Zn, Mo, Mn, Sn and other LIPs.

Notice that the resonance enhancement was realized in the single-atomic media presented in plasma. Different approaches were introduced to develop the theories adequately explaining the experimentally observed single-harmonic enhancement in such structures [6–8]. Meanwhile, the molecules-contained plasmas in most cases did not demonstrate this effect, in spite of using the molecular species containing the above-mentioned elements. This peculiarity was analyzed in [9].

In this paper, we consider atomic and molecular Cr-containing plasmas as the media for HHG. Our studies show the difference in the harmonic spectra retrieved from the plasmas comprising the atomic and molecular Cr-containing species. The detuning of strong ionic transitions and the decrease of their oscillator strengths in the molecular constituents are responsible for the suppression of resonance effect in molecular plasmas.

2. Results

Chromium (Cr), chromium oxide (Cr_20_3) and chromium carbide (Cr_3C_2) were used as the targets for laser plasma formation to generate high-order harmonics of ultrafast laser pulses.

#422269 https://doi.org/10.1364/OSAC.422269
Journal © 2021 Received 10 Feb 2021; revised 6 Mar 2021; accepted 22 Mar 2021; published 3 May 2021

OSA CONTINUUM

To create plasma, we used the Ti:sapphire laser (central wavelength 806 nm, pulse duration of uncompressed radiation 370 ps, pulse energy 6 mJ, 10 Hz pulse repetition rate). Part of amplified uncompressed radiation was separated from a whole beam and used as a heating pulse (HP) for LIP formation using the 200 mm focal length spherical lens installed in front of the 5-mm long target placed in the vacuum chamber (Fig. 1).

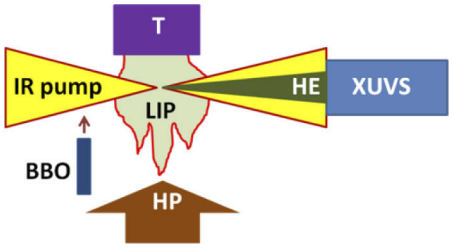

Fig. 1. Experimental setup for HHG in Cr-contained plasmas. IR pump: infrared (either 806 nm or tunable NIR) driving femtosecond pulses; BBO: nonlinear crystal (barium borate) for second harmonic generation used during two-color pump of plasmas; T: Cr-containing solid target; LIP: laser-induced plasma; HP: heating pulses; HE: harmonic emission; XUVS: extreme ultraviolet spectrometer.

In the case of single-color pump (SCP), the focused compressed (806 nm, 64 fs, 10 Hz) driving pulses (DP) with 120 µm focal spot size and intensity up to 5×10^{14} W cm^{-2} from this laser were aligned to propagate through LIP at a distance of ~200 µm above the target surface. The beta-barium borate (BBO) crystal was inserted into the vacuum chamber in the path of the 806 nm focused radiation to generate second harmonic for the two-color pump (TCP, 806nm+403 nm) of plasma.

We also used the optical parametric amplifier pumped by above-described laser to apply the tunable near infrared (NIR) radiation for HHG in LIP. In described experiments, only the signal pulses were used as DP for HHG. Most of experiments were carried out using the 1 mJ, 70 fs signal pulses tunable in the range of 1280–1440 nm. Most of experiments were carried out using the TCP of LIP. We used the second harmonic (H2) of signal pulses to apply the TCP scheme (NIR + H2) for HHG in plasma. The harmonic radiation was analyzed using an XUV spectrometer.

Figure 2 (upper panel) shows the plasma emission spectrum from Cr LIP at high fluence of HP (F=3 J cm^{-2}). One can see the numerous emission lines attributed to CrII-CrV ionic transitions. Such plasma contains high concentration of the free electrons, which destroy the phase-matching conditions for efficient harmonic generation due to the notable decrease of the coherence length of harmonics. Smaller fluence of HP (middle panel, F=1.9 J cm^{-2}) allowed for observation of the harmonic spectra up to the 33rd order (H33). One can see the gradual decay of harmonics between H11 and H25, while H27 almost disappeared from this spectrum. The appearance of strong H29 is a main feature of this harmonic distribution, which has earlier been reported in [10]. The rectangular boxes in this raw image point out the remaining weak emission lines from the chromium plasma. The concentration of free electrons at these conditions was significantly lower compared with the upper panel, which allowed generation of strong harmonics. Larger ratio between the enhanced H29 and lower orders was obtained at smaller fluence of HP (bottom panel, F=1.5 J cm^{-2}) when this harmonic dominated over all other harmonic orders down to H11. A decrease of lower-order harmonics yield in that case is attributed to smaller concentration of CrII ions responsible for harmonic generation.

In the case of TCP using 0.2 mm thick BBO, only a few weak even harmonics were observed alongside with odd ones. The application of 0.5 mm thick crystal in the case of HHG using TCP of chromium plasma significantly amended the yield of even harmonics and allowed for

OSA CONTINUUM

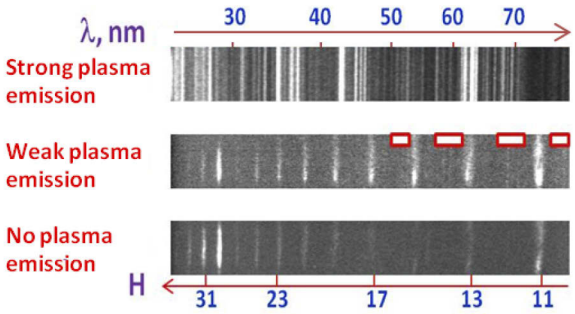

Fig. 2. Harmonic spectra from Cr plasma at different conditions of target formation and laser-plasma interaction using 806 nm laser radiation. (a) Plasma and harmonic spectra. Upper panel: plasma emission obtained at the fluence of heating pulses F=3 J cm^{-2}. Middle panel: harmonic spectrum and weak plasma emission spectrum obtained during ablation of chromium target using the fluence F = 1.9 J cm^{-2}. Weak plasma lines are seen in the spectral ranges marked by red boxes. Bottom panel: pure harmonic spectra without plasma emission at the fluence of heating pulses F=1.5 J cm^{-2}.

demonstration of approximately equal odd and even orders generation until the region where strong harmonics (H29 - H34) were obtained.

The photoabsorption and photoionization spectra of Cr plasma in the XUV range were previously analyzed in [11]. Those studies have demonstrated the presence of strong transitions of CrII, which could be responsible for the absorption of some harmonic orders in the wavelength region of 29.5–31 nm. Additionally, the $3p \rightarrow 3d$ transitions of CrII (27.6 - 28.2 nm, oscillator strength $gf = 0.63$) were analyzed in [12] and strongest ionic transitions that could enhance the nonlinear optical response of the plume were identified. Our studies, particularly demonstration of the suppression of H27 (λ=29.9 nm) and enhancement of H29 (λ=27.8 nm), corroborate with those predictions as well as with the theoretical analysis of HHG in chromium plasma reported in [13].

The application of the molecular targets containing chromium drastically changed the harmonic distribution. Below we show how the single harmonic enhanced in the case of atomic plasma completely lost this peculiarity once the chromium becomes a component of the molecular cloud produced during laser ablation.

Optimization of ablation conditions allowed significantly extending the cutoff of generating harmonics from the chromium plasma. Figure 3(a) shows the short-wavelength range of the harmonic spectrum produced during propagation of 806 nm pulses through the Cr LIP at the best conditions of plasma formation (F=1.5 J cm^{-2}). Term "best conditions" refers to those when largest difference between the resonance and non-resonance harmonics was achieved. Inset to this lineout presents the raw image of the shorter-wavelength part of XUV spectrum seen on the screen of CCD camera. We observed the harmonics up to H53. Similarly to Fig. 2, one can see a suppression of the 27th harmonic (λ=29.9 nm) followed by an enhancement of H29 (λ=27.8 nm).

Completely another pattern of harmonic distribution was observed in the case of SCP of Cr_3C_2 plasma when we observed a featureless gradually decayed spectrum of odd harmonics [Fig. 3(b)]. We did not observe the enhancement of harmonics in the vicinity of 27 nm. This spectrum was recorded at relatively weak fluence of HP (F=1.8 J cm^{-2}) for this target. Meanwhile, as soon as we increased the fluence of 370 ps heating pulses on the surface of the Cr_3C_2 target from 1.8 to 2.4 J cm^{-2}, the enhanced H29 appeared in the harmonic spectrum along with other lower- and higher-order odd harmonics [Fig. 3(c), thick blue curve]. Similar pattern was observed at these conditions of target ablation in the case of Cr LIP [Fig. 3(c), thin red curve]. The coincidence of the envelopes of harmonic distribution in these two cases, except for H27, which

OSA CONTINUUM

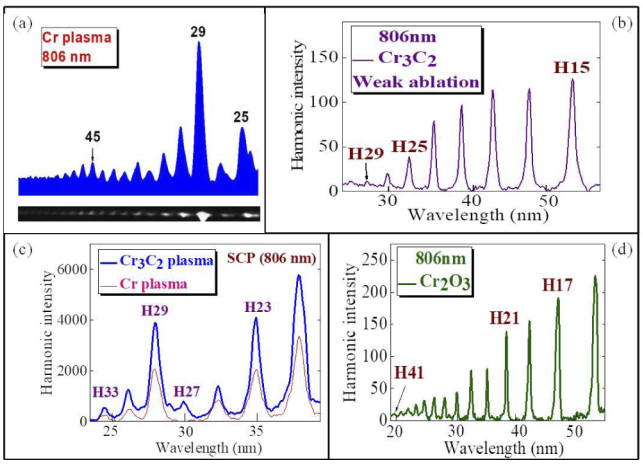

Fig. 3. Harmonic spectra from Cr, Cr_3C_2 and Cr_2O_3 plasmas using 806 nm driving pulses. (a) HHG in Cr LIP at the best conditions of plasma formation. Inset: raw image of this spectrum. (b) HHG in Cr_3C_2 plasma at weak ablation of chromium carbide (F=1.8 J cm^{-2}). H29 was not enhanced. (c) Comparative line-outs of harmonic distribution obtained from chromium (thin red curve) and chromium carbide (thick blue curve) at the fluence of heating pulses F=2.4 J cm^{-2}. H29 was enhanced in two plasmas. (d) HHG in Cr_2O_3 plasma at weak ablation of chromium oxide (F=1.8 J cm^{-2}). H29 was not enhanced. The growth of fluence on the chromium oxide target did not result in appearance of enhanced H29.

was absent in the case of ablated chromium target, point out the presence of the sufficient amount of similar atomic harmonic emitters in Cr and Cr_3C_2 LIPs. The appearance of a gain of single harmonic (H29) in the case of Cr_3C_2 plasma can be explained by the disintegration of this molecule at higher excitation into various components, among which the chromium ions can represent a sufficient amount of harmonic emitters. In that case HHG occurred in various plasma components. Accordingly, their harmonic spectra being merged will demonstrate the appearance of a single-harmonic gain attributed to the influence of the CrII $3p \rightarrow 3d$ transitions, as well as of H27 attributed to the generation from chromium carbide molecules.

In the meantime, another Cr-containing molecular target, Cr_2O_3, did not allow the observation of resonance-induced enhancement of harmonic, in spite of varying the fluence on the surface of this target. Figure 3(d) shows a typical spectral distribution of harmonics from chromium oxide plasma. This spectrum was recorded at weak ablation of chromium oxide (F=1.8 J cm^{-2}). One can see that H29 was not enhanced. The growth of fluence on the chromium oxide target up to F=2 J cm^{-2} did not result in appearance of enhanced H29. Further growth of fluence caused the generation of strong plasma emission and the decay of harmonic spectra. Probably, the disintegration of this molecule at suitable fluence of heating pulses did not provide a sufficient amount of CrII ions responsible for the resonance-induced enhancement of H29.

The application of SCP varying in a broad range (1280–1380 nm) did not allow generation of harmonics above 21st order (λ~64 nm), thus restricting the analysis of the variations of harmonic spectra in the shorter-wavelength region (26–30 nm). Because of this we analyzed the generated harmonics using TCP. We analyzed the harmonic emission spectrum in the case of propagation of 1300 nm pulses and second harmonic (650 nm) through the chromium plasma using the same optimal conditions of target ablation. The term "optimal conditions" refers to those allowing the observation of resonance-enhanced harmonic for the 806 nm pump [F=1.5 J cm^{-2}; Fig. 3(a)]. We observed the enhancement of a group of harmonics centered at H46 of 1300 nm radiation for which the resonance enhancement was assumed to be the best at the used experimental conditions.

OSA CONTINUUM

This spectral region well coincides with the one at which the enhancement of H29 and some higher-order harmonics of 806 nm radiation was achieved.

The tuning of NIR pulses in a broad range did not lead to the modification of the envelope of harmonic distribution from chromium LIP but rather changed the maximally enhanced harmonic. We observed the maximally enhanced harmonic (H49) of 1380 nm + 690 nm pump, with a few lower-order harmonics entirely absent in this spectrum, similarly to the case of H27 during application of 806 nm DP.

The short-wavelength harmonic spectrum using NIR driving radiation was completely changed as soon as we ablated the molecular targets containing chromium oxides and carbides at the conditions similar to HHG in atomic Cr plasma when we achieved a strong enhancement of single harmonic and some following harmonic orders. It is possible to foresee the preservation of resonant conditions for the metal component of this molecule. Accordingly, the amplification of a specific harmonic of NIR radiation during propagation through the chromium-contained molecules should also be achieved under the ablation conditions similar to the above-described experiments with a pure chromium target. However, in that case (i.e. at the fluence of heating pulses 1.5 J cm^{-2}) we observed a gradual decrease in each subsequent harmonic order and a smaller harmonic cutoff with regard to the Cr LIP [Figs. 4(a) and 4(b)]. We did not observe the enhanced harmonic in the region of 27–30 nm, like in the case of Cr LIP [Fig. 4(c)] while varying the ablation conditions of Cr_2O_3 and Cr_3C_2 targets up to F=2.2 J cm^{-2}). Larger fluencies of HP led to strong plasma emission and worsened conditions for HHG resulted in significant decrease of harmonic cut-off in the case of chromium oxide and chromium carbide LPs, similarly to the case of 806 nm experiments.

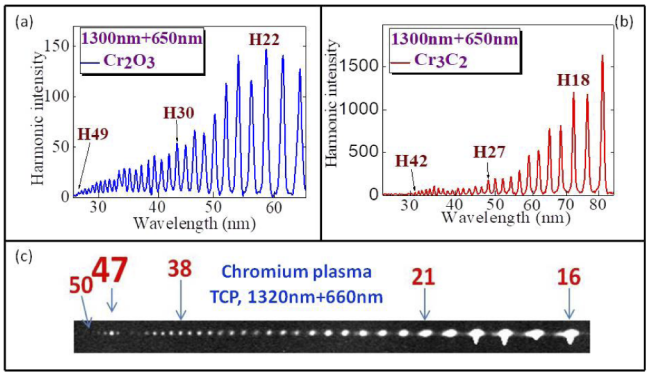

Fig. 4. Harmonic spectra from Cr_2O_3, Cr_3C_2 and Cr plasmas using tunable NIR driving pulses. (a) HHG in Cr_2O_3 LIP using 1300 nm + 650 nm driving pulses at best conditions of plasma formation. (b) HHG in Cr_3C_2 plasma using 1300 nm + 650 nm driving pulses at best conditions of plasma formation. (c) HHG in Cr plasma using 1320 nm + 660 nm driving pulses at best conditions of plasma formation.

3. Discussion

Here we address the variations of single-harmonic enhancement at different conditions of ablation of Cr target. A difference between the ratios of H29/H21 in Figs. 2 (bottom panel) and 3(c) can be explained as follows. Our studies showed that the ratio between "resonant" and "ordinary" harmonics decreases with the increase of the fluence of heating pulses. One can see this tendency once compares the raw images of spectra shown in Fig. 2 (middle and bottom panels). The application of larger fluence (middle panel, F=1.9 J cm^{-2}) decreased the ratio of yields of those harmonics (H29/H21) compared with the case of smaller fluence (bottom panel, F=1.5 J cm^{-2}).

OSA CONTINUUM

The ratio was changed from 10:1 to 4:1 for the 1.5 and 1.9 J cm^{-2} fluencies, respectively. The growth of fluence [F=2.4 J cm^{-2}, Fig. 3(c)] on the chromium target led to further decrease of this ratio (0.7:1). This conclusion is true for other non-resonant harmonics as well. Our studies showed that, with the growth of the fluence of heating pulses, the resonance enhancement of single harmonic becomes less pronounced due to the growing influence of the free electrons appearing in plasma at larger concentration. The destructive role of the latter species in harmonic generation is rather influential for resonance-enhanced harmonic compared with other orders in the plateau region of harmonics distribution. This difference in the role of restricting factors is due to the stronger influence of the group velocity dispersion of plasma on the phase-matching processes in the vicinity of ionic transitions possessing large oscillator strength compared with those out from such ionic transitions.

In Ref. 11, the absorption areas of C II in different ranges of extreme ultraviolet region were identified. Particularly, the 29.5–31 nm range was the one, which can cause the absorption of the harmonics generating in this region. The 27th harmonic of 806 nm radiation (λ=29.9 nm) lies in this region and the yield of this harmonic could be notably decreased compared with the neighboring harmonics that do not coincide with the areas of strong photoabsorption. The confirmation of the presence of notable absorption in the 29.3–31 nm range can also be found in Fig. 4©, where the raw image of generated spectrum shows a suppression of propagated emission between 43rd and 45th harmonics (29.3–30.7 nm) of 1320 nm radiation.

The disintegration of molecules leads to the appearance of the chromium ions in LIP. These ions allow for the resonant amplification in the vicinity of $3p \rightarrow 3d$ ionic transitions of Cr II. However, the use of various fluencies of HP on the surfaces of chromium carbide and chromium oxide targets did not lead to a strengthening of the harmonics in this region in the case of tunable NIR pump, which points out the insignificant amount of this component of disintegrated Cr_2O_3 and Cr_3C_2 molecules in LIP, contrary to the case when we used 806 nm driving pulses for generation of harmonics from the strongly ablated chromium carbide [Fig. 3(c)]. The absence of single-harmonic enhancement in the case of NIR DP can be attributed to the smaller HHG conversion efficiency using those pulses compared with 806 nm pump due to the $I_{\text{harm}} \propto \lambda^{-5}$ rule (I_{harm} is the harmonic intensity and λ is the driving field wavelength), which leads to a decrease of harmonic yield in the case of longer-wavelength sources compared with 806 nm pump. Meanwhile, the resonance enhancement of H47 was clearly achieved at different fluencies of heating pulses during propagation of 1320 nm radiation and its second harmonic through the plasma produced on the chromium target [Fig. 4(c)].

Our experiments using tunable NIR pulses showed that the shift of strong ionic transition in molecular plasmas plays insignificant role in the variation of the resonance effect (Fig. 4). The detuning of this transition in the case of molecules out from the atomic transition can be compensated for by tuning the wavelength of harmonic. However, these experiments showed that the fine tuning of harmonic along the expected strong transition did not result in the enhancement of some specific harmonics in the vicinity of this resonance.

The difficulties in formation of sufficient amount of atomic ions without destroying the suitable phase-matched conditions for harmonics generation were discussed in previous HHG studies using Zn-containing atomic and molecular plasmas [14]. Obviously, atomic singly-charged species can appear in plasma at stronger ablation conditions. However, the appearance of large amount of free electrons at these conditions of laser-induced ablation leads to the growing phase-mismatch between the interacting waves. Present studies using Cr-containing molecular species also demonstrated this feature thus restricting the enhancement of specific harmonic (29th order, in that case). The conclusion stating that laser ablation of strongly bound compound targets does not lead to the production of singly-charged atomic ions at sufficient densities required for resonance enhancement of specific high-order harmonics is applicable for the nanoparticle-containing plasmas as well. The analysis of the resonance enhancement of a

OSA CONTINUUM

single harmonic during propagation of ultrafast pulses through the atomic and nanoparticle tin-containing plasmas has also shown a notable distinction in the enhancement factor of the single harmonic in these two cases [15]. The enhancement of a single harmonic in the vicinity of the $4d^{10}5s^25p^2P_{3/2}\rightarrow 4d^95s^25p^2$ transition of Sn II ions demonstrated how this process depends on the constituency of the plasma components at different conditions of target ablation. Up to a 12-fold enhancement of even harmonic in the two-color pump of single-atomic Sn plasma followed by almost disappearance of resonance effect in the nanoparticle-containing tin plasma. Thus one can conclude that degradation of resonance-induced enhancement of nearby harmonic order in the non-atomic medium (molecules, nanoparticles) is a common feature distinguished from the harmonic amplification in the single-atomic species of similar elemental consistence.

Below we address the theoretical background of resonance-induced harmonic enhancement. The evaluation of the relative advantages and disadvantages of analytical as well as numerical methods in the case of resonant high-harmonic generation has recently been introduced in [16]. Initially, this process firstly reported in the case of HHG in LIP [17] was attributed to the multiple recolliding electron trajectories. Then, after revealing a similar correspondence between experimental resonance-enhanced HHG enhancements in plasmas [18–24] and transitions with high oscillator strengths between the ground state and autoionizing state (AIS) of the generating ions [25], the "four-step model" of resonant HHG was introduced. This model extended the three-step model [26] by including the resonant harmonic emission along with the 'classic', nonresonant one. The first two steps of the four-step model — (i) tunnelling ionization, and (ii) free-electron motion — were the same as in the three-step model. Then, if the energy of the electron returning back to the parent ion is close to the one of the AIS transitions, the third step of the three-step model turns into two: (iii) electron capture into the AIS, and (iv) relaxation from the AIS down to the ground state, accompanied by the XUV emission. This model well explained the experimental observations of resonance-enhanced single harmonics in LIPs.

Meanwhile, a number of attempts to create other models describing resonant HHG were made. Those were based on bound-bound transitions [27–29], as well as on a connection of the multi-electron excited states to the enhanced yield of harmonics [6,7,13,30]. A high-order harmonic generation theory, which generalizes the strong-field approximation to the resonant case when the harmonic frequency is close to that of the transition from the ground state to an autoionizing state of the generating system, is presented in [31]. Each of those models describes, to some extent, the resonance-related HHG experiments in LIPs. Our experimental results in the case of atomic Cr plasma well match with the theoretical consideration of this process described in the above refereed theoretical studies independent of the wavelength of pumping laser, thus confirming the generalized approach of those theoretical studies.

Summarizing, the existing theories of the microprocess of resonance-induced enhancement of a single harmonic in atomic plasmas are mostly based on (i) the four-step model, (ii) the harmonic generation in the presence of a shape resonance using time-frequency analysis of the intensity and phase, which underlined the resonance enhancement irrespective of the pulse length and supported the four-step model, and (iii) the approach generalized for the case when the capture into an AIS is replaced by the field-induced excitation of the ground state into this state. The usual three-step scenario that applies the factorization formula without additional assumptions [7] also provides explanation of the earlier reported resonance-enhanced processes in different LIPs, as well as those studied in present research of atomic Cr plasmas. The variation of target excitation broadens analysis of the nonlinear response of such plasma by comparing the enhancement of different harmonics provided they coincide or stay close to those resonances. In particular, the application of this approach during numerical study of HHG in Zn ions allowed the resonance effect in harmonic generation to be observed due to transitions to the highly excited bound states, rather than to the AIS [23]. However, these bound states are broader due to photoionization in the intense laser field. Thus in this sense there is no fundamental difference between transitions

OSA CONTINUUM

to AIS (enhancing above-ionization threshold harmonics) and transitions to highly excited bound states (enhancing below-threshold harmonics). Moreover, the generation of the below-threshold harmonics also includes the quasi-free electronic motion as one of the steps of the process, and therefore the resonant enhancement of this generation can be described within the similar four-step model. One has to take into consideration the opportunity in competition of the micro- and macro-processes in the LIP. In particular, the comparison of the quasi-phase matching and resonance enhancement of harmonics using TCP of plasmas has been demonstrated and discussed in [32].

Notice that the aforementioned resonance enhancement has clearly been demonstrated both experimentally and theoretically only in the case of atomic plasmas. Meanwhile, the application of the molecular plasmas contained the components responsible for amplification process did not result in resonantly-enhanced single harmonic, in spite of the attempts to decay and disintegrate molecules without destroying the phase-matching conditions. Previous calculations of the modified HHG spectra in the case of different plasmas were performed to distinguish the level of detuning and the mechanisms that lead to a decrease in the amplification of a specific harmonic order in the case of a molecular plume with respect to an atomic one [9]. The discrepancy between the calculated spectra and the experimentally observed less effective resonance-induced amplification of harmonics in semiconductor molecules compared with atomic/ionic plasmas was explained by a significantly greater influence of the strong electric field of laser radiation on the symmetry and dynamic modification of the molecular spectra in LIP.

In previous simulations of HHG in LIPs [33], an effective Coulomb potential (e.g., soft-core potential) was adopted to mimic the target. For the atomic Cr-containing plasma reported in the present study, one can choose a similar method as in [33], and strong emission can be obtained in the simulations. On the other hand, in principle, one should also choose the similar method for Cr-containing molecular plasmas. However, in the case of similar potential, the same strong emission of single harmonic from above molecular LIPs is anticipated which is in contrast with our experiment. To explain our experimental findings in molecular chromium-containing plasmas, more sophisticated theory such as density functional theory will be needed to accurately simulate the target structures and dynamics.

4. Conclusions

In conclusion, we have re-examined the resonance enhancement of single-harmonic emission during propagation of ultrafast pulses through the chromium-containing plasmas. We have compared the atomic (Cr) and molecular (Cr_2O_3, Cr_3C_2) plasmas to demonstrate a distinction in the enhancement factor of the single harmonic or the group of enhanced shorter-wavelength harmonics. We have shown how, in the case of 806 nm pump, the enhancement of 29^{th} harmonic (λ=27.8 nm) in Cr-contained plasma depends on the constituency of the plasma components at different conditions of target ablation. The application of tunable (1280–1440 nm) radiation from optical parametric amplifier allowed demonstrating the notable variations (from 46^{th} to 49^{th} order) of single-harmonic enhancement using two-color pump of Cr plasma. Meanwhile, no enhancement of harmonics was observed in the case of chromium carbide and chromium oxide plasmas, except for the case of overexcited Cr_3C_2 plasma and 806 nm pump. This approach in studying the high-order nonlinear processes in different plasmas allows predicting the modification of the resonance-induced single harmonic enhancement earlier reported in other single-atomics plasmas (manganese, selenium, zinc, indium, tin, tellurium, molybdenum, arsenic, etc.) being presented in the molecular form.

Funding. State Assignment to Higher Educational Institutions of Russian Federation (FZGU-2020-0035); European Regional Development Fund (1.1.1.5/19/A/003); Japan Society for the Promotion of Science (24760048).

Disclosures. The authors declare no conflicts of interest.

OSA CONTINUUM

Data availability. Data underlying the results presented in this paper are not publicly available at this time but may be obtained from the authors upon reasonable request.

References

1. R. A. Ganeev, H. Singhal, P. A. Naik, U. Chakravarty, V. Arora, J. A. Chakera, R. A. Khan, M. Raghuramaiah, S. R. Kumbhare, R. P. Kushwaha, and P. D. Gupta, "Optimization of the high-order harmonics generated from silver plasma," Appl. Phys. B **87**(2), 243–247 (2007).
2. Y. Pertot, L. B. Elouga Bom, V. R. Bhardwaj, and T. Ozaki, "Pencil lead plasma for generating multimicrojoule high-order harmonics with a broad spectrum," Appl. Phys. Lett. **98**(10), 101104 (2011).
3. C. Hutchison, R. A. Ganeev, T. Witting, F. Frank, W. A. Okell, J. W. G. Tisch, and J. P. Marangos, "Stable generation of high-order harmonics of femtosecond laser radiation from laser produced plasma plumes at 1 kHz pulse repetition rate," Opt. Lett. **37**(11), 2064–2066 (2012).
4. R. A. Ganeev, M. Suzuki, and H. Kuroda, "Quasi-phase-matching of high-order harmonics in multiple plasma jets," Phys. Rev. A **89**(3), 033821 (2014).
5. M. Singh, M. A. Fareed, A. Laramée, E. Isgandarov, and T. Ozaki, "Intense vortex high-order harmonics generated from laser-ablated plume," Appl. Phys. Lett. **115**(23), 231105 (2019).
6. D. B. Milošević, "Resonant high-order harmonic generation from plasma ablation: Laser intensity dependence of the harmonic intensity and phase," Phys. Rev. A **81**(2), 023802 (2010).
7. M. V. Frolov, N. L. Manakov, and A. F. Starace, "Potential barrier effects in high-order harmonic generation by transition-metal ions," Phys. Rev. A **82**(2), 023424 (2010).
8. V. Strelkov, "Role of autoionizing state in resonant high-order harmonic generation and attosecond pulse production," Phys. Rev. Lett. **104**(12), 123901 (2010).
9. R. A. Ganeev and P. V. Redkin, "Role of resonances in the high-order harmonic enhancement in diatomic molecules," Opt. Commun. **281**(15-16), 4126–4129 (2008).
10. R. A. Ganeev, M. Suzuki, M. Baba, and H. Kuroda, "Harmonic generation in XUV from chromium plasma," Appl. Phys. Lett. **86**(13), 131116 (2005).
11. C. McGuinness, M. Martins, P. Wernet, B. F. Sonntag, P. van Kampen, J.-P. Mosnier, E. T. Kennedy, and J. T. Costello, "Metastable state contributions to the measured 3p photoabsorption spectrum of Cr+ ions in a laser-produced plasma," J. Phys. B **32**(20), L583–L591 (1999).
12. J. B. West, J. E. Hansen, B. Kristensen, F. Folkmann, and H. Kjeldsen, "Revised interpretation of the photoionization of Cr+ in the 3p excitation region," J. Phys. B **36**(19), L327–L333 (2003).
13. R. A. Ganeev, S. Odžak, D. B. Milošević, M. Suzuki, and H. Kuroda, "Resonance enhancement of harmonics in metal plasmas using tunable mid-infrared pulses," Laser Phys. **26**(7), 075401 (2016).
14. R. A. Ganeev and H. Kuroda, "High-order harmonics generation in atomic and molecular zinc plasmas," Photonics **8**(2), 29 (2021).
15. R. A. Ganeev and H. Kuroda, "Reexamining different factors of the resonance-enhanced high-order harmonic generation in atomic and nanoparticle laser-induced tin plasmas," Appl. Sci. **11**(5), 2193 (2021).
16. G. S. J. Armstrong, M. A. Khokhlova, M. Labeye, A. S. Maxwell, E. Pisanty, and M. Ruberti, "Dialogue on analytical and ab initio methods in attoscience," https://arxiv.org/abs/2101.09335.
17. R. A. Ganeev, M. Suzuki, M. Baba, H. Kuroda, and T. Ozaki, "Strong resonance enhancement of a single harmonic generated in the extreme ultraviolet range," Opt. Lett. **31**(11), 1699–1701 (2006).
18. M. Suzuki, M. Baba, R. Ganeev, H. Kuroda, and T. Ozaki, "Anomalous enhancement of a single high-order harmonic by using a laser-ablation tin plume at 47 nm," Opt. Lett. **31**(22), 3306–3308 (2006).
19. M. Suzuki, M. Baba, H. Kuroda, R. A. Ganeev, and T. Ozaki, "Intense exact resonance enhancement of single-high-harmonic from an antimony ion by using Ti:Sapphire laser at 37 nm," Opt. Express **15**(3), 1161–1166 (2007).
20. R. A. Ganeev, P. A. Naik, H. Singhal, J. A. Chakera, and P. D. Gupta, "Strong enhancement and extinction of single harmonic intensity in the mid- and end-plateau regions of the high harmonics generated in weakly excited laser plasmas," Opt. Lett. **32**(1), 65–67 (2007).
21. R. A. Ganeev, L. B. E. Bom, J.-C. Kieffer, and T. Ozaki, "Systematic investigation of resonance-induced single-harmonic enhancement in the extreme-ultraviolet range," Phys. Rev. A **75**(6), 063806 (2007).
22. R. A. Ganeev, V. V. Strelkov, C. Hutchison, A. Zaïr, D. Kilbane, M. A. Khokhlova, and J. P. Marangos, "Experimental and theoretical studies of two-color pump resonance-induced enhancement of odd and even harmonics from a tin plasma," Phys. Rev. A **85**(2), 023832 (2012).
23. R. A. Ganeev, M. Suzuki, S. Yoneya, V. V. Strelkov, and H. Kuroda, "Resonance enhancement of harmonics in laser-produced Zn II and Zn III containing plasmas using tunable mid-infrared pulses," J," Phys. B **49**(5), 055402 (2016).
24. V. V. Kim, G. S. Boltaev, M. Iqbal, N. A. Abbasi, H. Al-Harmi, I. S. Wahyutama, T. Sato, K. L. Ishikawa, R. A. Ganeev, and A. S. Alnaser, "Resonance enhancement of harmonics in the vicinity of 32 nm spectral range during propagation of femtosecond pulses through the molybdenum plasma," J," Phys. B **53**(19), 195401 (2020).
25. G. Duffy and P. Dunne, "The photoabsorption spectrum of an indium laser produced plasma," J," Phys. B **34**(6), L173–L178 (2001).

OSA CONTINUUM

26. P. B. Corkum, "Plasma perspective on strong field multiphoton ionization," Phys. Rev. Lett. **71**(13), 1994–1997 (1993).
27. E. S. Toma, P. Antoine, A. D. Bohan, and H. G. Muller, "Resonance-enhanced high-harmonic generation," J," Phys. B **32**(24), 5843–5852 (1999).
28. M. B. Gaarde and K. J. Schafer, "Enhancement of many high-order harmonics via a single multiphoton resonance," Phys. Rev. A **64**(1), 013820 (2001).
29. C. Figueira de Morisson Faria, R. Kopold, W. Becker, and J. M. Rost, "Resonant enhancements of high-order harmonic generation," Phys. Rev. A **65**(2), 023404 (2002).
30. D. B. Milošević, "High-energy stimulated emission from plasma ablation pumped by resonant high-order harmonic generation," J," Phys. B **40**(17), 3367–3376 (2007).
31. V. V. Strelkov, M. A. Khokhlova, and N. Yu Shubin, "High-order harmonic generation and Fano resonances," Phys. Rev. A **89**(5), 053833 (2014).
32. R. A. Ganeev, G. S. Boltaev, S. Y. Stremoukhov, V. V. Kim, A. V. Andreev, and A. S. Alnaser, "High-order harmonic generation during different overlaps of two-colored pulses in laser-produced plasmas," Eur. Phys. J. D **74**(10), 199 (2020).
33. R. A. Ganeev, Z. Wang, P. Lan, P. Lu, M. Suzuki, and H. Kuroda, "Indium plasma in the single- and two-color mid-infrared fields: Enhancement of tunable harmonics," Phys. Rev. A **93**(4), 043848 (2016).